30th Annual International IEEE EMBS Conference
Vancouver, British Columbia, Canada, August 20-24, 2008

Regional Differences in Rabbit Atrial Action Potential Properties: Mechanisms, Consequences and Pharmacological Implications

Oleg V. Aslanidi, Rebecca S. Dewey, Alexandra R. Morgan, Mark R. Boyett and Henggui Zhang

Abstract—**Regional differences in electrical action potential (AP) properties can provide a substrate for atrial arrhythmias. We quantify such differences by developing detailed AP models for the left (LA) and right (RA) rabbit atrial cells in order to study the underlying electrophysiological mechanisms, as well as their impacts on vulnerable properties of the atrial tissue. The transient outward current, I_{to}, is identified as the major factor contributing to the AP differences between the LA and RA cells, which suggests a potential pharmacological target for reducing heterogeneity and vulnerability of the atria.**

I. Introduction

COMMON cardiac arrhythmias, such as atrial flutter and fibrillation (AF), are associated with irregular reentrant electrical activity in the heart [1, 2]. Both experimental and computational evidence supports the idea that cardiac (primarily, atrial) tissues with large regional differences in electrical properties are more vulnerable to reentry [3, 4], which may result from unidirectional conduction block in regions with longer refractoriness. However, relationships between the atrial electrical heterogeneity and vulnerability to reentry are difficult to dissect experimentally.

Biophysically detailed computational models have been successfully used to dissect mechanisms of complex cardiac dynamics observed in experiments, and results obtained with small animal models have been commonly applied to explain respective behavior in humans [5-7]. The aim of this study is to construct and study detailed computer models accounting for electrophysiological differences between the LA and RA [8, 9]. A generic rabbit atrial AP model [10] is modified based on extant voltage-clamp datasets recorded for several major ionic currents (I_{Na}, I_{CaL}, I_{Kr}, I_{Ks}, I_{K1} and I_{to}) from the rabbit atria [11-16]. The resultant single-cell AP models are incorporated into 1D tissue models in order to simulate the AP propagation, and quantify the relationships between electrical heterogeneity and vulnerability of the rabbit atrial tissue, as well as pharmacological impacts that can be used to control them.

Manuscript submitted April 16, 2008. This work was supported by a project grant from the Biotechnology and Biological Sciences Research Council (BBS/B/1678X), United Kingdom.

O. V. A. Author is with the School of Physics and Astronomy, University of Manchester, Manchester M13 9PL, United Kingdom (tel: +44-161-200-3966; e-mail: oleg.aslanidi@manchester.ac.uk).

R. S. D. Author is with the School of Physics and Astronomy, University of Manchester, Manchester M13 9PL, United Kingdom (e-mail: rebecca.dewey@student.manchester.ac.uk).

A. R. M. Author is with the School of Physics and Astronomy, University of Manchester, Manchester M13 9PL, United Kingdom (e-mail: alexandra.morgan@student.manchester.ac.uk).

M. R. B. Author is with the Faculty of Medicine and Human Sciences, University of Manchester, Manchester M13 9NT, United Kingdom (e-mail: mark.boyett@.manchester.ac.uk).

H. Z. Author is with the School of Physics and Astronomy, University of Manchester, Manchester M13 9PL, United Kingdom (e-mail: henggui.zhang@manchester.ac.uk).

II. Methods

A. Model Development

The dynamics of electrical activation in cardiac tissues can be described by the following well-known equation [6, 7]:

$$\frac{\partial V}{\partial t} = \nabla \cdot \mathrm{D} \nabla V - \frac{I_{\mathrm{ion}}}{C_m} \,. \qquad (1)$$

Here V (mV) is the membrane potential, ∇ is a spatial gradient operator, t is time (s), D is a diffusion coefficient ($mm^2\ ms^{-1}$) that characterizes electrotonic spread of voltage via gap junctional coupling, I_{ion} is the total membrane ionic current (pA), and C_m (pF) is the membrane capacitance.

A biophysically detailed model describing individual ionic currents comprising I_{ion} for a rabbit atrial cell has been developed by Lindblad et al. [10]. It accurately reproduces the voltage-clamp data on which it has been based, and provides feasible morphologies of the rabbit atrial AP, but has some limitations: (i) it uses hybrid experimental datasets from cells in the rabbit LA, the sinoatrial node and the ventricles; (ii) it ignores regional differences in the electrical properties of atrial cells. However, APs in rabbit LA and RA cells have different morphologies and rate-dependence [8].

We develop a new family of AP models for the rabbit LA and RA cells that (i) is based on experimental data obtained from rabbit atrial cells, and (ii) incorporates details of regional differences in cell electrical properties. First, the Lindblad et al. model [10] is modified in order to incorporate available experimental data [11-16] for the kinetics of major ionic currents from rabbit atrial cells (Fig. 1). Second, ionic differences in between the LA and RA cells are introduced (see below) based on experimental measurements [8, 9]. All equations for the LA and RA single cell models can be found at http://personalpages.manchester.ac.uk/staff/H.Zhang-3/.

Eq. (1) is used to simulate AP propagation in respective 1D atrial tissues. The diffusion coefficient is set to the value $D = 5\ mm^2\ ms^{-1}$, which produces the AP conduction velocity of ~0.5 m/s, as seen in experiments [17]. Eq. (1) is solved using the explicit Euler's method with time and space steps $\Delta t = 0.005$ ms and $\Delta x = 0.1$ mm, respectively.

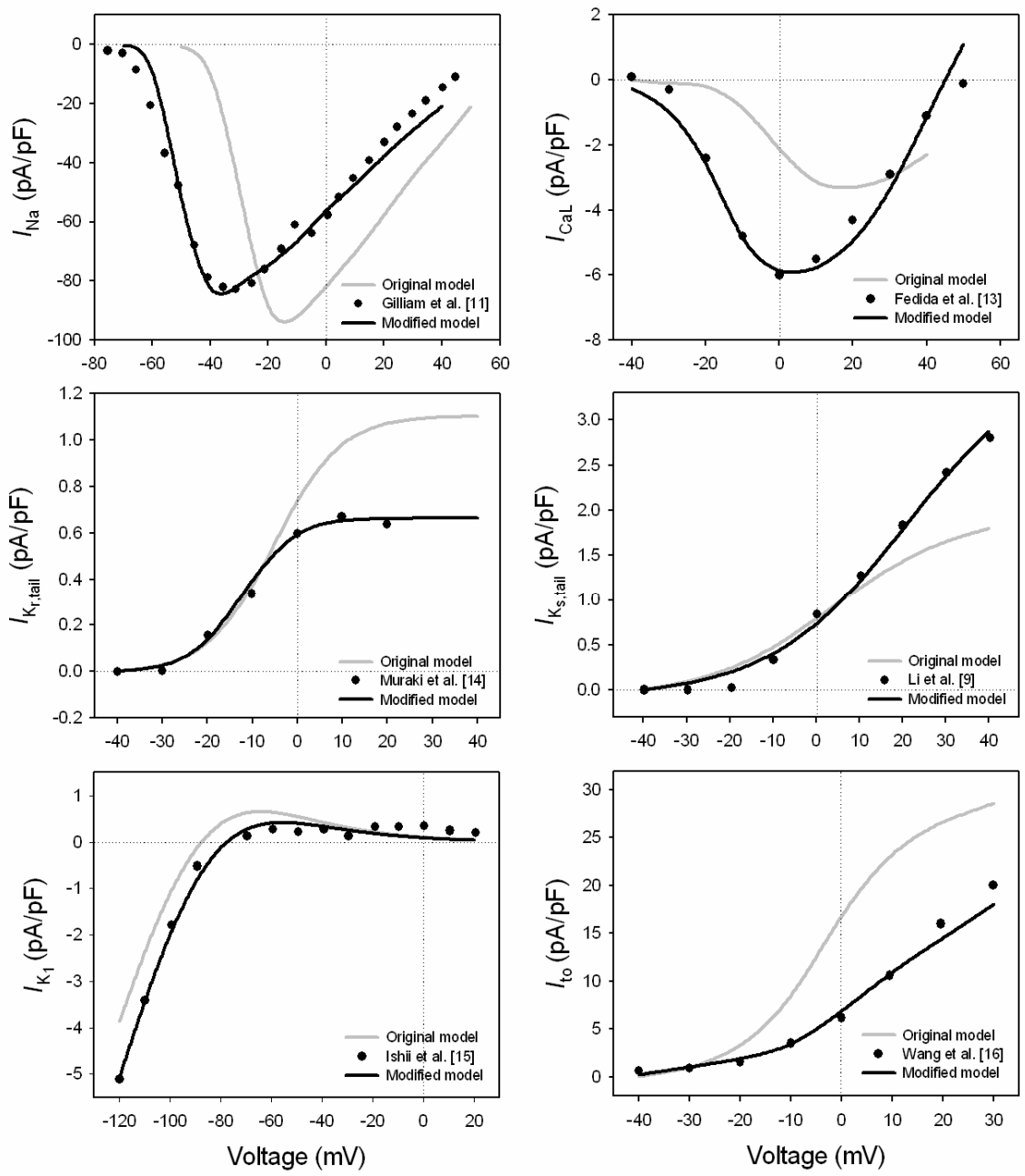

Fig. 1. Current-voltage (I-V) relationships for several major ionic currents in a rabbit atrial cell computed from the original model [10], our modified model and measured in experiments (references are in respective panels). Simulated I-V curves (solid lines) are plotted along with the respective experimental data (dots). Note that the current density of I_{Na} was adjusted to reproduce recent experimental data recorded at 37^0 [12].

B. Atrial Heterogeneity

Fig. 1 summarizes properties of major ionic currents – I_{Na}, I_{CaL}, I_{Kr}, I_{Ks}, I_{K1} and I_{to} – in both the LA and RA models. Differences between the LA and RA were introduced based on experimental data obtained from rabbit [8] and dog [9].

Detailed studies of canine atrial cells [9] have shown insignificant differences in current densities of I_{CaL}, I_{Ks}, I_{K1} and I_{to} between the LA and RA. Reported small differences in the current density of I_{Kr} – it is ~30% higher in LA than in RA – produced minor differences in the AP duration when incorporated into the model. However, large variations of the AP morphologies have been reported between the rabbit LA and RA [8]. The AP differences progressively increased as the pacing cycle length was increased from 500 to 2000 ms, but were almost completely eliminated by 4-AP, a selective blocker of the transient outward K^+ current, I_{to} [8].

Hence, as the atrial AP heterogeneity shows strong rate-dependence only in the presence of I_{to} [8], but its current density does not vary between the LA and RA [9], the atrial heterogeneity can be attributed to differences in the kinetics of I_{to}. Rate-dependence of I_{to} is well-known [18, 19], and is determined by time constants of inactivation and reactivation (recovery from inactivation) of this current. Both time constants have fast and slow components: in rabbit atrial

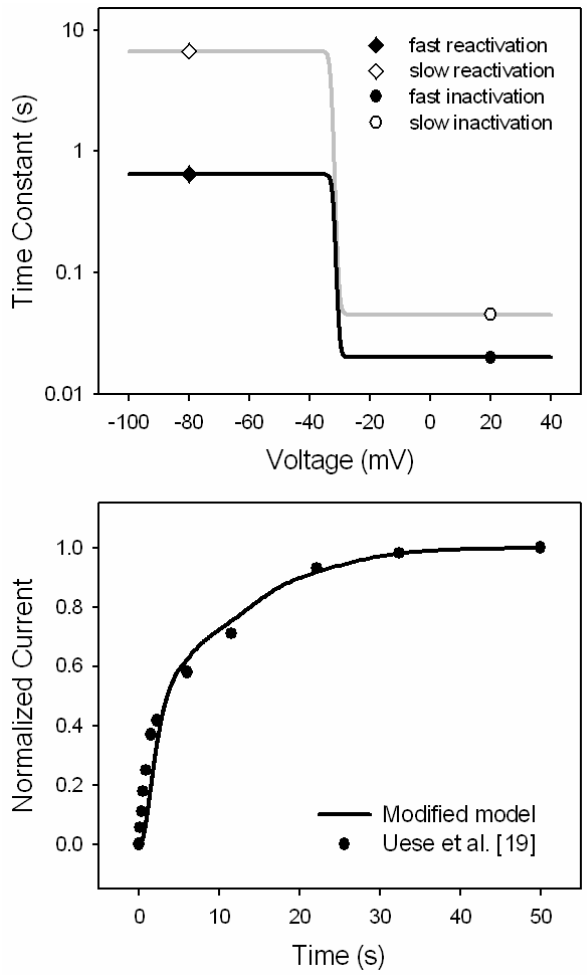

Fig. 2. Kinetics of the transient outward current, I_{to}. Top: Fast and slow inactivation time constants (black and grey lines, respectively) are modeled as sigmoid curves connecting respective discrete values (symbols) for fast/slow inactivation times measured experimentally at +20 mV [16, 19], and fast/slow reactivation times measured at -80 mV [18, 19]. Bottom: rate-dependence of I_{to}; a simulated curve (solid line) is plotted along with the respective experimental data (dots). I_{to} progressively increases as the pacing cycle length is increased [19].

cells the fast and slow inactivation time constants vary in the range 10-25 ms and 40-260 ms, respectively [16, 19]; the fast and slow reactivation time constants vary in the range 500-1600 ms and 6600-8400 ms, respectively [18, 19].

Fig. 2 shows incorporation of the inactivation/reactivation time constants into the model, and resultant rate-dependence of I_{to}. Slow inactivation and reactivation time constants were set to values 45 and 6650 ms, respectively, in both the LA and RA models. Fast inactivation and reactivation time constants were set to values 20 and 650 ms in the LA, and 20 and 1250 ms in the RA. Thus, major heterogeneity between the LA and RA was assumed in the fast reactivation time constant. Below we show that this was sufficient to produce remarkably different AP rate-dependence in the LA and RA.

III. Results

Fig. 3 illustrates APs simulated using the developed LA and RA models. The AP morphologies and rate-dependence are in a very good agreement with experimental data [8]. In the LA, both the AP duration and plateau are significantly decreased when the basic cycle length (BCL) is increased from 500 to 1000, and then 2000 ms – whereas responses to similar BCL changes in the RA are much smaller. These differences are eliminated when I_{to} in the models is blocked (not shown, AP morphologies in both atria in this case are very similar to the respective APs in control simulations at BCL = 500 ms, but with slightly elevated plateaus), which reproduces experimentally observed effects of 4-AP, a selective I_{to} blocker, in the rabbit LA and RA [8].

AP propagation in 1D models of the LA and RA tissues was simulated in order to study effects of the atrial AP heterogeneity on vulnerability of the tissue. Fig. 4 shows refractory periods (RPs) and vulnerable windows measured in control simulations of the LA and RA tissues, as well as respective simulations of the effects of 4-AP and AVE0118 – a blocker of both the transient current, I_{to}, and its sustained component, I_{sus} [20]. AVE0118 has been used to stop AF by increasing refractoriness of atrial tissue – simulations show a similar increase of the RP with AVE0118, but not with 4-AP. However, the vulnerable window was equally decreased in both 4-AP and AVE0118 simulations. Both drugs also decreased rate-dependence of the tissue vulnerability.

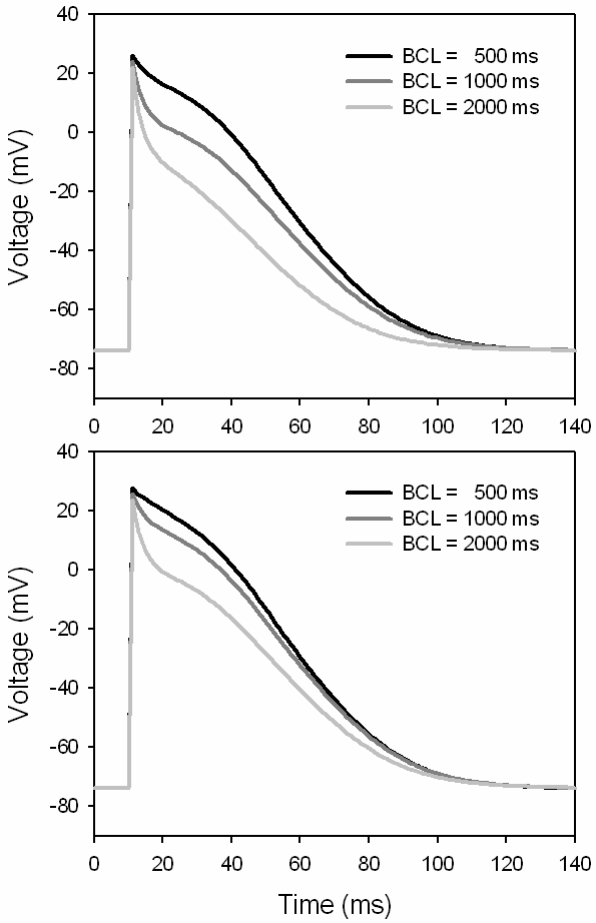

Fig. 3. Rate-dependence of APs simulated with the LA and RA cell models (top and bottom, respectively). AP morphologies match the respective experimental recordings presented in Fig. 7 by Qi et al. [8].

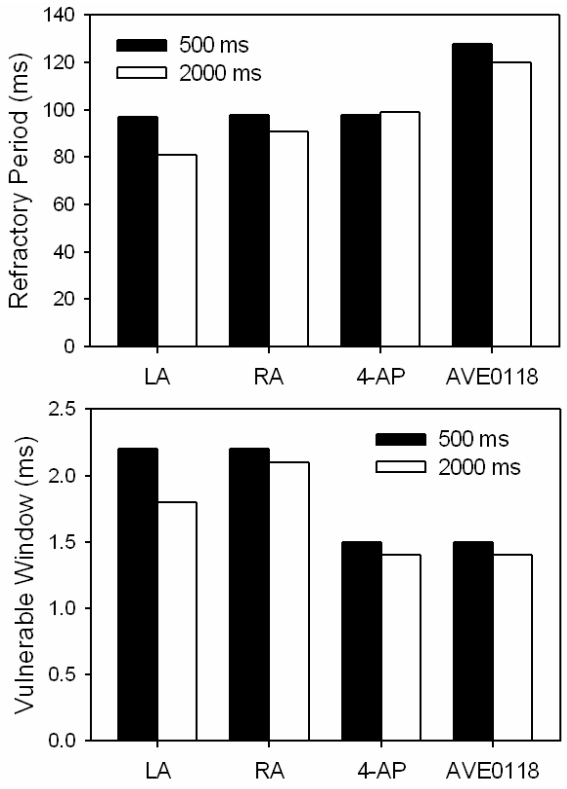

Fig. 4. Refractoriness and vulnerability of atrial tissues. Tissues were paced 5 times at the BCL of 500 or 200 ms before the standard S1-S2 protocol [7] was applied in order to measure the vulnerable window of S2-pulse intervals resulting in unidirectional AP conduction block. RP was defined as the maximum S2 interval that failed to initiate AP conduction. The effect of AVE0118 was simulated by decreasing conductance of the background outward current I_{sus} [10] by 50% in addition to 100% block of I_{to}. Note that simulations of both I_{to} blockers (4-AP and AVE0118) produced similar results for both LA and RA tissues, as I_{to} accounted for major differences between them.

IV. Conclusion

We have developed a new family of AP models for the LA and RA cells, which incorporates experimental data on atrial electrical properties [8-16]. Experimentally reported AP differences between the LA and RA [8] were accounted for by different fast inactivation time constants of the transient outward current, I_{to}, in these two cell types. This provided a mechanistic explanation for different AP morphologies and rate-dependence between the LA and RA. Note that similar approach has been successfully used to simulate transmural AP heterogeneity in the ventricles [7]. 1D models were used to study vulnerability of the LA and RA tissues and evaluate pharmacological impacts modulating it. Blocking I_{to} by 4-AP or AVE0118 enabled reduction of the atrial heterogeneity and the vulnerable window, whereas additional effects of AVE0118 on I_{sus} increased refractoriness of the tissue. Hence, compared to most class III drugs that increase tissue heterogeneity and vulnerable window [7], the atrial-specific drug AVE0118 [20] is both effective and relatively safe, and therefore, may provide a potential agent for pharmacological treatment of atrial arrhythmias in human patents.

References

[1] S. Nattel, D. Li, and L. Yue. "Basic mechanisms of atrial fibrillation - very new insights into very old ideas". *Ann. Rev. Physiol.*, vol. 62, pp. 51-77, 2000.

[2] J. Jalife, O. Berenfeld, and M. Mansour. "Mother rotors and fibrillatory conduction: a mechanism of atrial fibrillation". *Cardiovasc. Res.*, vol. 54, pp. 204-16, 2002.

[3] M.A. Allessie, F.I. Bonke, and F.T.G. Schopmann. "Circus movement in rabbit atrial muscle as a mechanism of tachycardia. II. The role of nonuniform recovery of excitability in the occurrence of unidirectional block studied with multiple microelectrodes". *Circ. Res.*, vol. 39, pp. 168-77, 1976.

[4] M.S. Spach, P.C. Dolber, and J.F. Heidlage. "Interaction of inhomogeneities of repolarization with anisotropic propagation in dog atria: a mechanism for both preventing and initiating reentry". *Circ. Res.*, vol. 65, pp. 1612-31, 1989.

[5] R.A. Gray, A.M. Pertsov, and J. Jalife. "Spatial and temporal organization during cardiac fibrillation". *Nature*, vol. 392, pp. 75-78, 1998.

[6] Z.L. Qu, K. Kil, F.G. Xie, A. Garfinkel, and J.N. Weiss. "Scroll wave dynamics in a three-dimensional cardiac tissue model: Roles of restitution, thickness, and fiber rotation". *Biophys. J.*, vol. 78, pp. 2761-75, 2000.

[7] A.P. Benson, O.V. Aslanidi, H. Zhang, and A.V. Holden. "The canine virtual ventricles: a platform for dissecting pharmacological effects on propagating and arrhythmogenesis". *Prog. Biophys. Mol. Biol.*, vol. 96, pp. 187-208, 2008.

[8] A. Qi, J.A. Yeung-Lai-Wah, J. Xiao, and C.R. Kerr. "Regional differences in rabbit atrial repolarization: importance of transient outward current". *Am. J. Physiol.*, vol. 266, pp. H643-49, 1994.

[9] D. Li, L. Zhang, J. Kneller, and S. Nattel. "Potential ionic mechanism for repolarization differences between canine right and left atrium". *Circ. Res.*, vol. 88, pp.1168-75, 2001.

[10] D.S. Lindblad, C.R. Murphey, J.W. Clark, and W.R. Giles. "A model of the action potential and underlying membrane currents in a rabbit atrial cell". *Am. J. Physiol.*, vol. 271, pp. H1666-96, 1996.

[11] F.R. Gilliam, C.F. Starmer, and A.O. Grant. "Blockade of rabbit atrial sodium channels by lidocaine. Characterization of continuous and frequency-dependent blocking". *Circ. Res.* vol. 65, pp. 723-39, 1989.

[12] J.H. Ko, W.S. Park, S.J. Kim, and Y.E. Earm. "Slowing the inactivation of voltage-dependent sodium channels by staurosporine, the protein kinase C inhibitor, in rabbit atrial myocytes". *Eur. J. Pharmacol.*, vol. 534, pp. 48-54, 2006.

[13] D. Fedida, Y. Shimoni, and W.R. Giles. "Alpha-adrenergic modulation of the transient outward current in rabbit atrial myocytes". *J. Physiol.*, vol. 423, pp. 257-77, 1990.

[14] K. Muraki, Y. Imaizumi, M. Watanabe, Y. Habuchi, and W.R. Giles. "Delayed rectifier K^+ current in rabbit atrial myocytes". *Am. J. Physiol.*, vol. 269, pp. H524-32, 1995.

[15] Y. Ishii, K. Muraki, A. Kurihara, Y. Imaizumi, and M. Watanabe. "Effects of sematilide, a novel class III antiarrhythmic agent, on membrane currents in rabbit atrial myocytes". *Eur. J. Pharmacol.*, vol. 331, pp. 295-302, 1997.

[16] Z. Wang, J. Feng, H. Shi, A. Pond, J.M. Nerbonne, and S. Nattel. "Potential molecular basis of different physiological properties of the transient outward K^+ current in rabbit and human atrial myocytes". *Circ. Res.*, vol. 84, pp. 551-61, 1999.

[17] J.R. de Groot, T. Veenstra, A.O. Verkerk, et al. "Conduction slowing by the gap junctional uncoupler carbenoxolone". *Cardiovasc. Res.*, vol. 60, pp. 288-97, 2003.

[18] B. Fermini, Z. Wang, D. Duan, and S. Nattel. "Differences in rate dependence of transient outward current in rabbit and human atrium". *Am. J. Physiol.*, vol. 263, pp. H1747-54, 1992.

[19] K. Uese, N. Hagiwara, T. Miyawaki, and H. Kasanuki. "Properties of the transient outward current in rabbit sino-atrial node cells". *J. Mol. Cell. Cardiol.*, vol. 31, pp. 1975-84, 1999.

[20] S. de Haan, M. Greiser, E. Harks, Y. Blaauw, A. van Hunnik, S. Verheule, M. Allessie, and U. Schotten. "AVE0118, blocker of the transient outward current $I_{(to)}$ and ultrarapid delayed rectifier current $I_{(Kur)}$, fully restores atrial contractility after cardioversion of atrial fibrillation in the goat". *Circulation*, vol. 114, pp. 1234-42, 2006.